VIBRATION STUDIES OF DEEP GROOVE BALL BEARING WITH SINGLE DEFECT ON BALL AND OUTER RACES

[1]Vishal G. Salunkhe, [2]Vishwajit S. Hubale, [3]Mahesh H. Arbune
[1]Assistant Professor, [2]Undergraduate, [3]Undergraduate
Department of Mechanical Engineering
Annasaheb Dange College of Engineering and Technology Ashta.
Pin: 416 301, Maharashtra, India.

Abstract : Ball bearing is widely used in different industries where high speed and low load operations are performed. Due to the catastrophic failure of bearing the whole process in the industry may be stopped, maybe an accident happen. Due to all situations, major loss is heath and money. To reduce the losses in this paper we are doing vibration analysis of ball bearing has a single defect on ball and defect on outer race. Also have given try on simulation in ANSYS with different load and defect conditions.

***Keywords*:** defect on ball, defect on outer races, mathematical model, amplitude, simulation.

I. INTRODUCTION

A bearing is a machine element that constrains relative motion to only the desired motion and reduces friction between moving parts. There are various types of bearings according to applications. Roller bearings are used in industries for heavy load applications and ball bearings are used for domestic as well as high speed industrial applications. Deep groove ball bearings are particularly versatile. They are suitable for high and very high speeds, accommodate radial and axial loads in both directions and require little maintenance. Because of this deep groove ball bearings are the most widely used bearing. Ball bearings are widely used in small to big industrial machines. Performances of such machines are greatly influenced by quality of bearings used in it. Despite the perfect geometry of ball bearings, vibrations are commonly generated through the interaction of the rolling elements during motion. Rolling bearings during operation may generate localized defects viz. cracks, pits, spalls, etc., primarily due to fatigue of mating surfaces. Unnoticed local defects in their early stages may result in progressively higher noise and vibrations and finally leading to the failure of the rotor-bearing system causing severe economic and personal losses. Thus, detection of local defects is an important task and research subject from a condition monitoring point of view.

The studies carried out by various researchers related to the vibration analysis of defects in bearing are described here. Patel and Tandon [1] developed a dynamic model for the study of vibrations of deep groove ball bearings having single and multiple defects on surfaces of inner and outer races. The authors considered the masses of shaft, housing, races and balls in the modeling. They obtained the governing equation by using Runga-Kutta method. The developed model provides the vibrations of shaft, balls and housing in the time and frequency domain. kalman and Dutt [2] presented the kalman filtering algorithm for the clearer detection of defect frequencies related to bearing faults. The authors find out there is sufficient potential I using the Kalman filter as an effective tool to denoise the bearing vibration signal.

II. Experimental details :

The experimental setup shown in Fig. 1 is designed and fabricated to investigate the vibration characteristics of ball bearings. Experimental setup has electrical motor which vary speed from 0 rpm to 2000rpm. Shaft is used having diameter 20mm and length 800mm. Ball bearings are used having inner diameter 30 mm. For the assembly of bearing and shaft 25mm outer diameter and 20mm inner diameter sleeve is used. The used sleeve has taper 1:12 this gives easy replacement of bearing. Coupling is used to connect shaft and motor. Whole setup is placed on rubber cushion to reduce vibrations. Load is acted on shaft at the middle. Load arrangement is also shown in fig.no.1 following table 1 shows specifications of bearing.

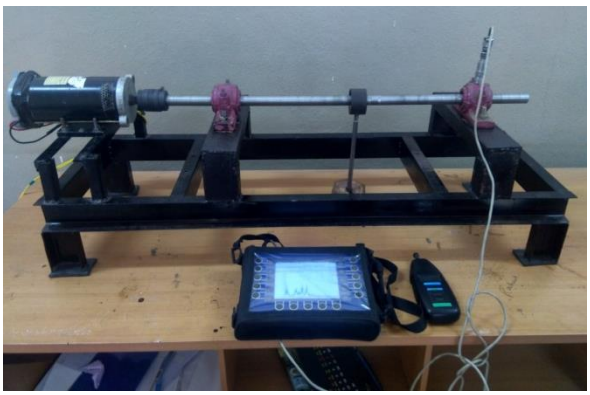

Fig.no.1

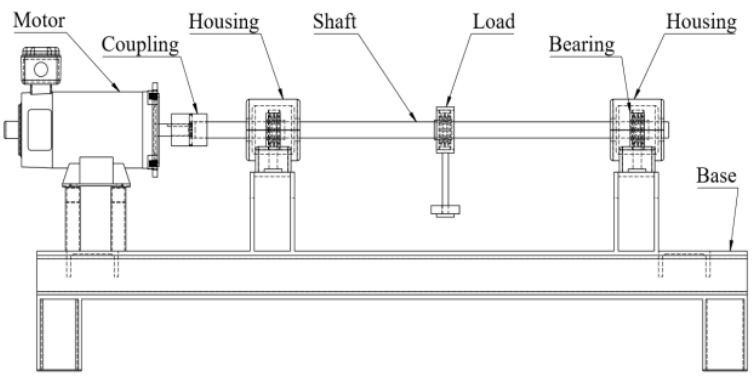

Fig.no.2

Vibration analyses are done by FFT analyzer. The accelerometer is placed on housing with position horizontal and vertical this gives reading of vibration amplitudes. The schematic diagram of experimental setup is shown in fig.2.

Table 1 Deep groove ball bearings available in market

Inner Diameter of the bearing (d)	= 30 mm
Outer Diameter of the bearing (D)	= 62mm
Width of the bearing (B)	= 19mm
Dynamic load capacity (C)	= 21.50 kN
Static load capacity (C_o)	= 7.40 kN
Bearing material	=High-grade bearing steel

For the experimentation we create defect on ball and outer races by using EDM. The size of defect varies in range 0.5mm*0.5mm0.5mm, 1mm*1mm*1mm, 1.5mm, 1.5mm*1.5mm, 2mm*2mm*2mm, 2.5mm*2.5mm*2.5mm. This size defect in ball and races means we have 5 ball defect bearing and 5 outer race defect bearings. The defects are shown in fig.3

Defect on Ball Defect on outer race

Fig. no. 3

III. Result and Discussion:

First we perform experiment on healthy bearing. Then driving end side bearing is healthy and non-driving side bearing is replaced with defected bearing. For these conditions we changed speed from 500rpm to 1250rpm in step of 250rpm. For healthy bearing : For healthy bearing following signatures are taken on FFT for various speed conditions at a constant load i.e. 20 N. Velocity value is measured on Y-axis whereas X-axis shows vibrational frequencies of the bearing. Below fig. shows the FFT reading at speed 500 rpm only and the graph shows the variation in velocity values with respect to speed change.

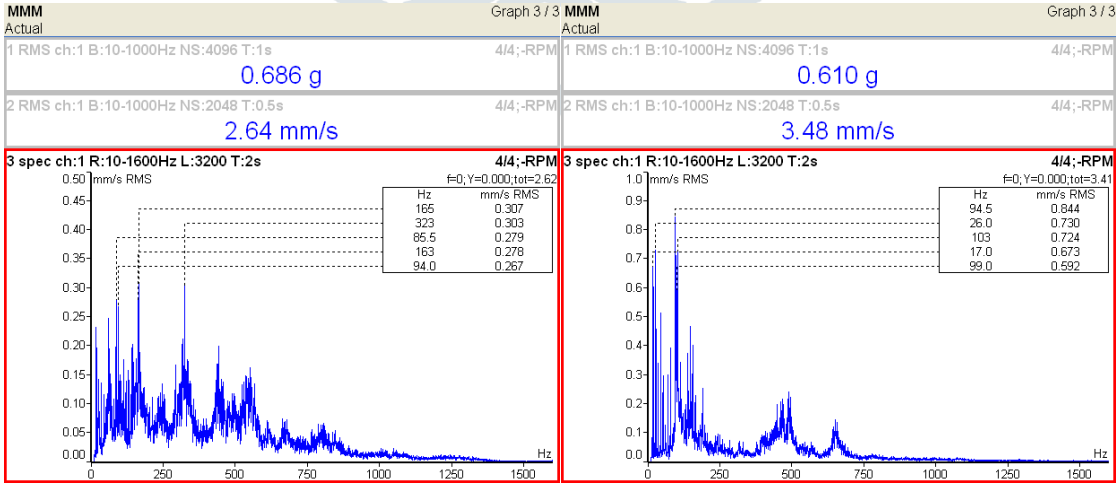

Horizontal location Vertical location

Fig.no.4

Figure 4 shows the vibration spectra for the healthy bearing located at DE and NDE, under constant load and varying speed conditions. While the x axis shows the vibrational frequencies of the bearing, the y axis represents velocity values. The frequency spectra are showing some small peaks are due to inherent bearing characteristics. These peaks have very low values of vibration amplitudes, thus indicating that the bearing is a healthy bearing. The frequency spectra plot in Figure 4 may be used as a baseline reference for further work. In addition, the frequency spectra exhibit some other frequencies which may be attributed to the flexibilities involved in structure of the test rig.

Next for non-driving side bearing is replaced by defected bearing. For each defected bearing 4 speeds range 500rpm, 750rpm, 1000rpm and 1250rpm. For all this conditions horizontal and vertical locations amplitude is measured. Means for 1 defect 4 different speed and 2 locations. Like this total defected bearing count is 10. It is not possible to put all the screenshots of FFT in this paper. So below graph shows amplitude values at different load and different speed.

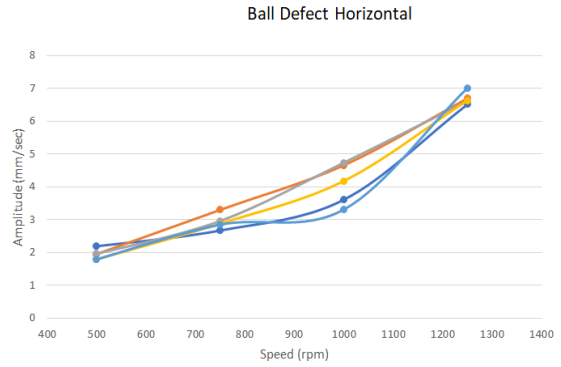

Figure 5 Defect on Ball (Horizontal location)

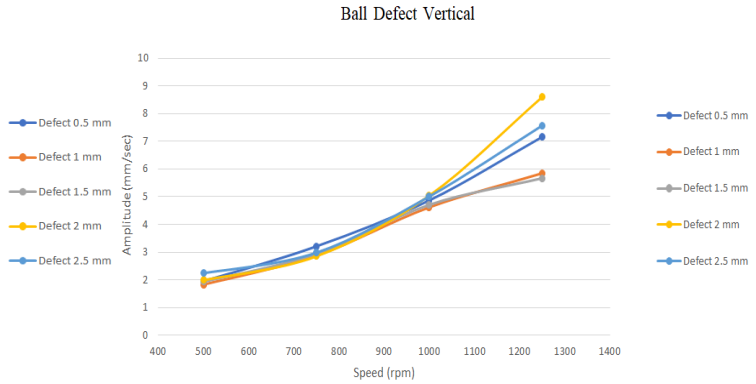

Figure 6 Defect on Ball (Vertical location)

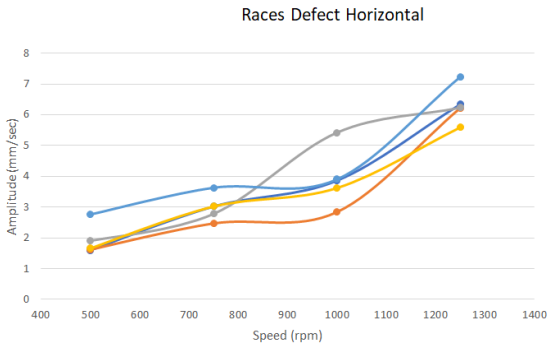

Figure 7 Defect on Race (Horizontal location)

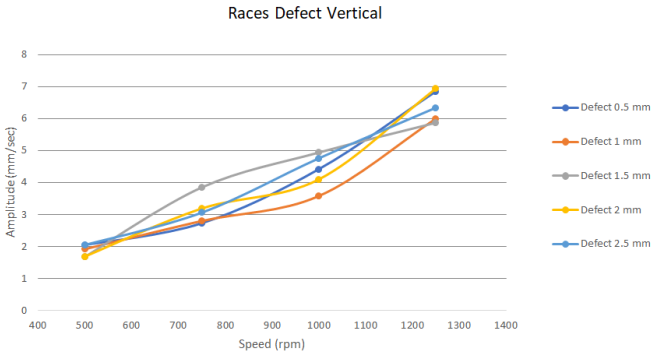

Figure 8 Defect on Race (Vertical location)

By observing all the above figures (for defect on ball as well as defect on outer race at both location horizontal and vertical) we can conclude that as defect size increases and speed increases amplitude increases. The highest amplitude is at defect size 2.5mm*2.5mm*2.5mm and speed 1250 rpm.

IV. Simulation

In the simulation part we considered one ball and their respective portion of outer races as shown in fig.9. This simulation is performed on ANSYS WORKBENCH. Load is directly acted on ball in downward direction.

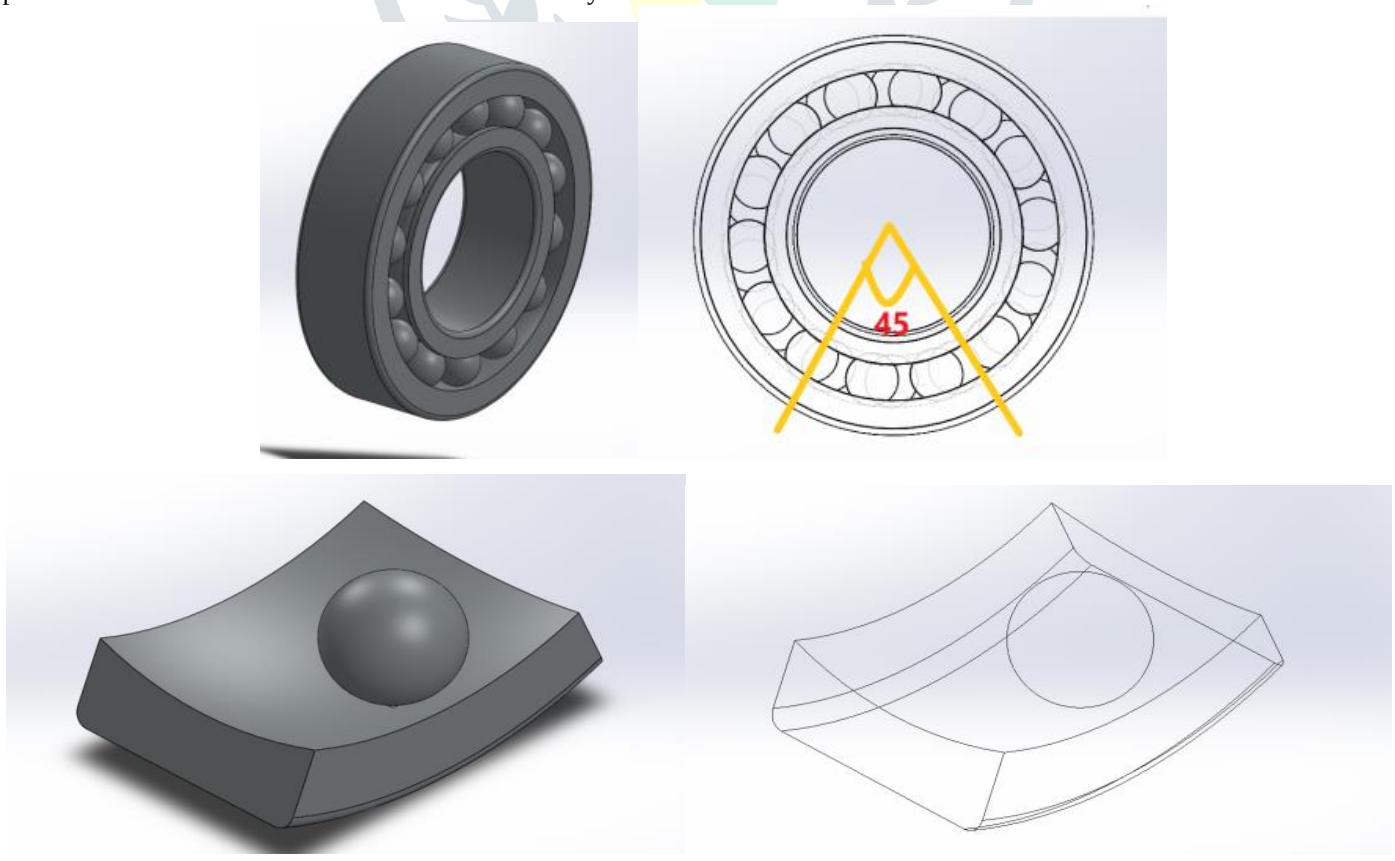

Figure 9

Specification of bearing is as follows.
Bearing 1206 K, Inner diameter 30 mm, Outer diameter = 62 mm, Width = 16 mm, No. of balls = 28, Diameter of ball = 7.94 mm and material used for Bearing is Chrome Steel. Properties of chrome steel is mentioned in following table

Table 2

Parameters	Values
Density	7810 Kg/m^3
Young's modulus	2.016E+05 MPa
Bulk Modulus	1.4E+05 MPa
Possion's ratio	0.26
Shear modulus	80000 MPa
Tensile Yield Strength	415 MPa
Ultimate Tensile Strength	520 MPa

The simulations are performed with defect on ball, defect on ball with some angle and defect on outer races.

1) Defect on ball :

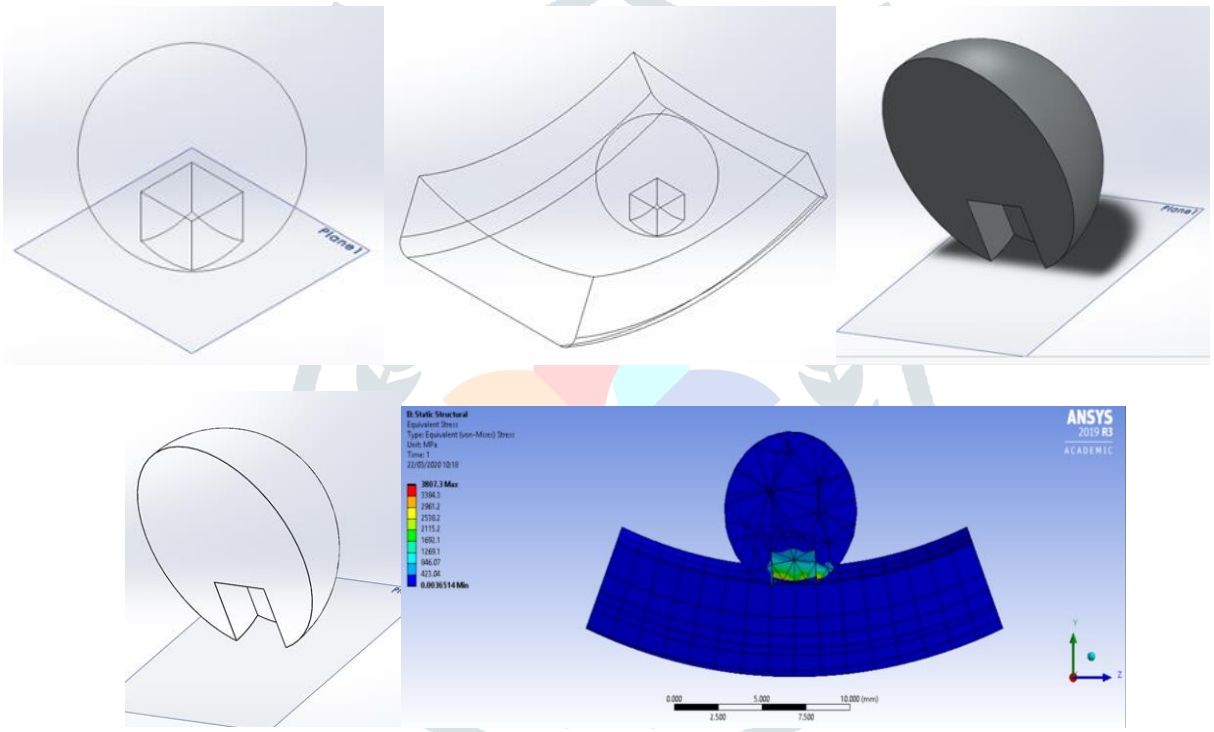

Figure 10

Now with varying load on ball and varying defect size simulations are performed. This simulation gives the stresses generated in area of contact and deformation at the point of contact. Following graph no.1 and 2 gives the results of simulation. The defect is square shaped and size varies as follows 0.5mm*0.5mm*0.5mm,1mm*1mm*1mm, 1.5mm*1.5mm*1.5mm,2mm*2mm*2mm, 2.5mm*2.5mm*2.5mm and load varies in a range of 100N, 200N, 300N, 400N, 600N, 800N, 1000N.Deformation is given in mm and stress is in MPa.

By observing below graph no. 1 we can say that deformation increases as load increases and defect size increases. The highest deformation is at load 1000N and defect size is 2.5mm*2.5mm*2.5mm. By observing graph no.2 we can say that stresses induced in the contact surfaces is increases as increases load and increases defect size. The highest stresses generated at a load 1000N and defect size is 2.5mm*2.5mm*2.5mm.

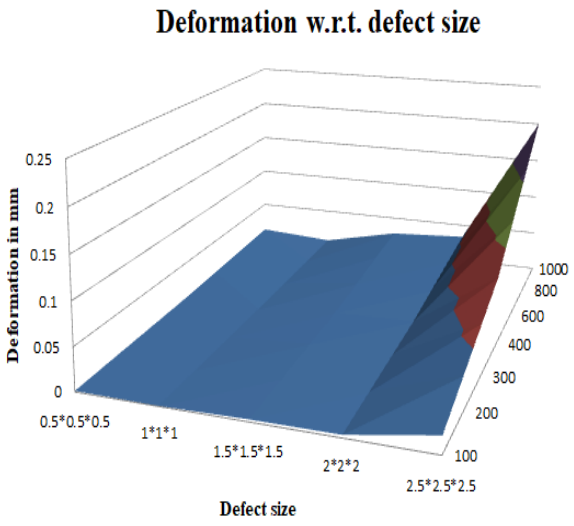

Graph no.1

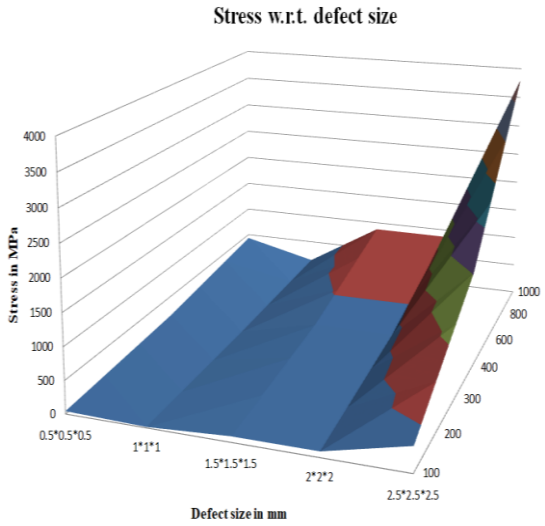

Graph no.2

2) Defect on ball with angle :

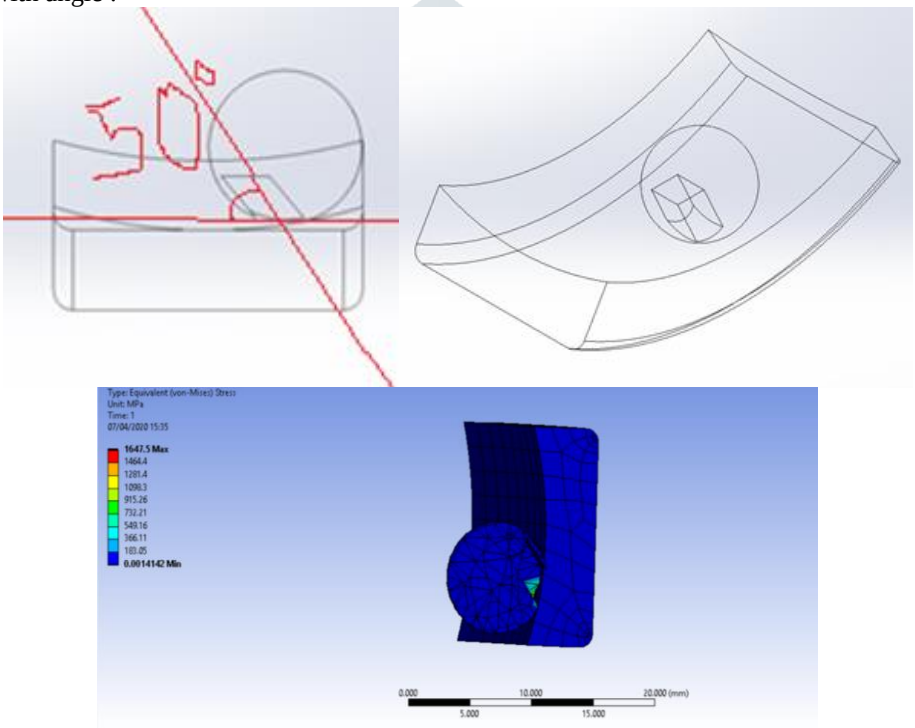

Figure 11

Now with varying load on ball and varying angle of defect on ball simulations are performed. This simulation gives the stresses generated in area of contact and deformation at the point of contact. The defect is square shaped and size 2.5mm*2.5mm*2.5mm with angle 50º, 60º , 70º , 80º , 90º , 100º , 110º , 120º and load varies in a range of 100N, 200N, 300N, 400N, 600N, 800N, 1000N. Deformation is given in mm and stress is in MPa. Following graph no.3 and 4 gives the results of simulation.

By observing below graph no. 3 we can say that deformation increases as load increases and angle of defect increases. The highest deformation is at load 1000N and defect angle is 120º. By observing graph no.4 we can say that stresses induced in the contact surfaces is increases as increases load and angle of defect increases but at angle 60º to 80º and load 100 N to 300N stress are high. The highest stresses generated at a load 1000N and at angle 120º

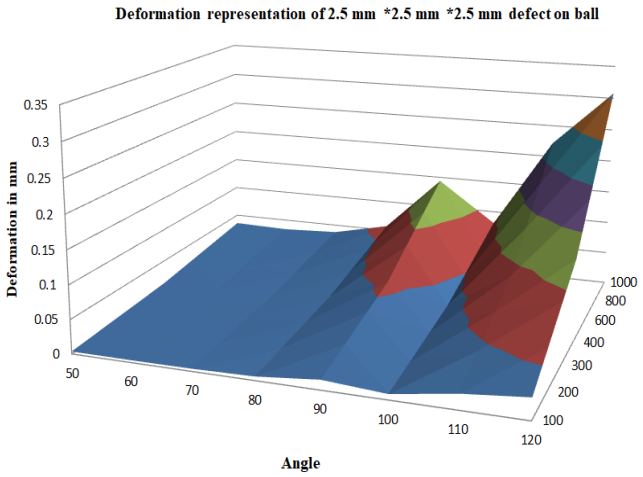

Graph no, 3

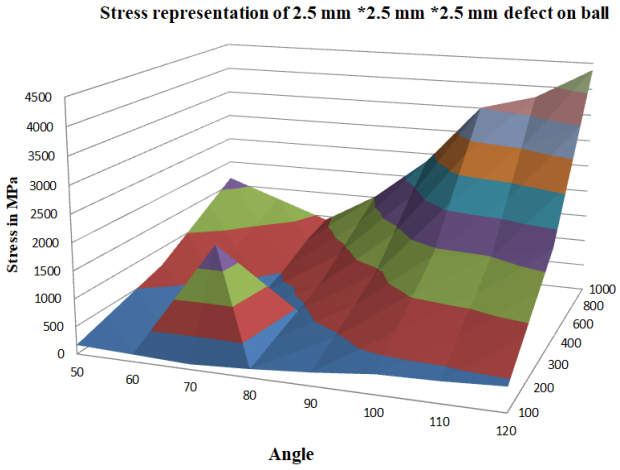

Graph no. 4

3) Defect on Outer Race:

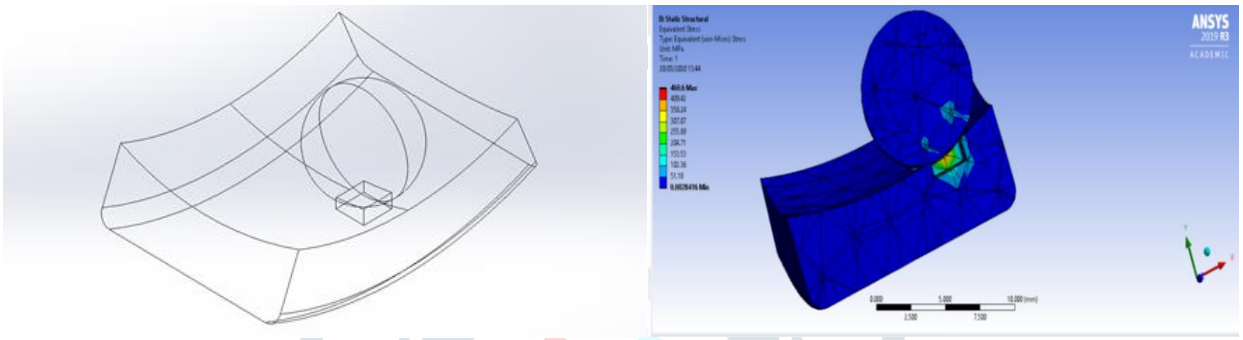

Fig.no.12

Now with varying load on ball and varying depth of defect on race simulations are performed. This simulation gives the stresses generated in area of contact and deformation at the point of contact. The defect is square shaped and size 2.5mm*2.5mm with different depth size 0.25mm,0.75mm,1.25mm,1.75mm and load varies in a range of 100N, 200N, 300N, 400N, 600N, 800N, 1000N. Deformation is given in mm and stress is in MPa. Following graph no.5 and 6 gives the results of simulation.

By observing below graph no. 5 we can say that deformation increases as load increases and depth up to 0.75mm after this depth increases deformation decreases. The highest deformation is at load 1000N and at 0.75mm depth of defect. By observing graph no.6 we can say that stresses induced in the contact surfaces is increases as increases load and depth up to 0.75mm after this depth increases stress decreases .The highest stresses generated is at load 1000N and at 0.75mm depth of defect.

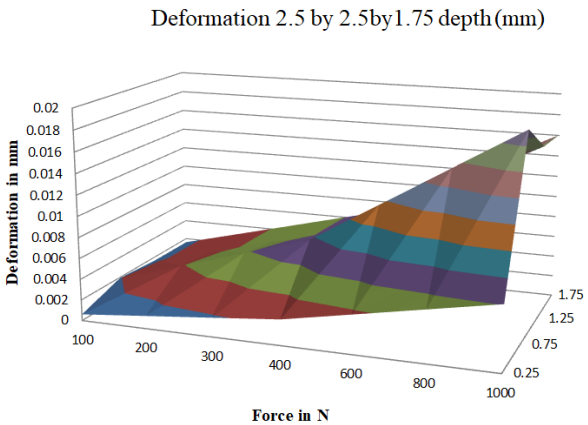

Graph no. 5

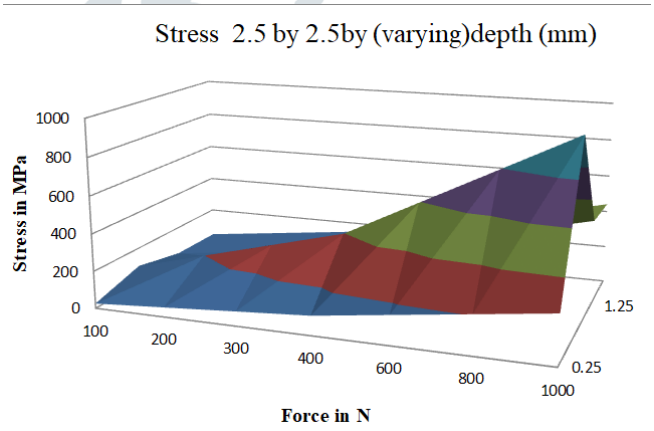

Graph no. 6

4) Defect on race with depth 0.25mm:

Now with varying load on ball and taking constant depth 0.25mm let us compare with non-defective bearing. Size of defect varies in range of 0.5mm*0.5mm*0.25mm, 1mm*1mm*0.25mm,1.5mm*1.5mm*0.25mm,2mm*2mm*0.25mm,2.5mm*2.5mm*0.25mm and load increases in range of 100N, 200N, 300N, 400N, 600N, 800N, 1000N.Following graph no. 7 and 8 gives results of simulation.

By observing below graph no. 7 we can say that deformation increases as load increases and size increases up to 1.5mm*1.5mm*0.25mm and then deformation decreases. The highest deformation is at load 1000N and at defect size 1.5mm*1.5mm*0.25mm. By observing graph no.8 we can say that stresses induced in the contact surfaces is increases as increases load and size increases up to 1.5mm*1.5mm*0.25mm and then stress decreases. The highest stresses generated is at load 1000N and at defect size 1.5mm*1.5mm*0.25mm.

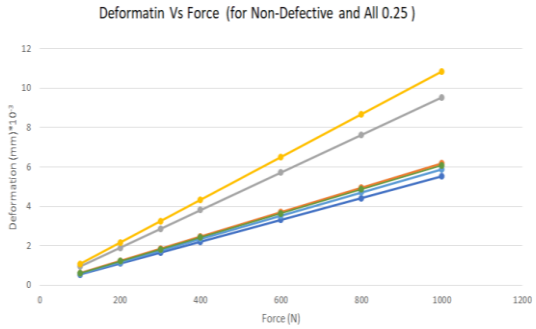

Graph no.7

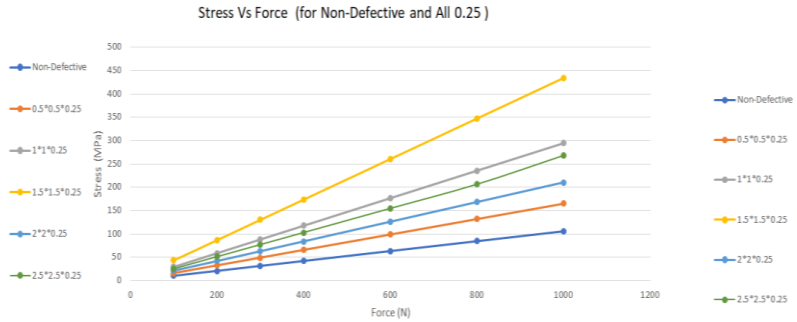

Graph no.8

V. Concluding Remarks:

Deep groove ball bearings having defects in outer race and rolling element defect has been studied. Defects are created on outer race and rolling element (ball) by using EDM. Vibration response of faulty bearing measured with the help of FFT for various speed. The frequency domain approach is used and absolute values are taken during measurement. The following conclusions are drawn from this research work:

1. From experimental data, it is concluded that for healthy bearing there is less vibration level is observed.
2. With increase in defect size; both in the case of on ball and outer race defect, vibration amplitude increases. {With increase in defect size; both in the case of on ball and outer race defect, vibration amplitude fluctuates.}
3. In 50 % of cases [different defect sizes, speeds and bearing element], experimental frequencies are closely matching. For remaining cases, deviation in the frequencies may be due to variation in the clearance between bearing elements namely inner race, outer race and ball.
4. Good correlations between simulation model and experimental results amply demonstrate that this model may be used with confidence for the study and prediction of vibration amplitude of healthy and defective bearings.
5. Stress and deformation increases as size of defect increases as well as load increases for both conditions defect on ball and defect on outer race.

   In other case of defect on race with increasing depth of defect deformation and stress increases as load increases but up to depth 0.75mm after this as depth increases deformation and stress decreases.

Reference:

[1]	Patel, V. N., Tandan, N., and Pandey, R. K., 2010, "A Dynamic Model for Vibration Studies of Deep Groove Ball Bearings Considering Single and Multiple Defects in Races," ASME J. Tribol., 132, p. 041101.
[2]	Khanam, S., Dutt, J. K.,Tandon, N.,2014, "Extracting Rolling Element Bearing Faults From Noisy Vibration Signal Using Kalman Filter" J. of Vibration and Acoustics by ASME , Vol. 136 pp. 256-265.
[3]	Babu, C. K., Tandon, N., Pandey, R. K.,2014, "Nonlinear Vibration Analysis of an Elastic Rotor Supported on Angular Contact Ball Bearings Considering Six Degrees of Freedom and Waviness on Balls and Races" J. of Vibration and Acoustics by ASME Vol. 136 pp. 657-667.
[4]	Patel, V. N., Tandon, N., Pandey, R. K., 2013 "Vibration Studies of Dynamically Loaded Deep Groove Ball Bearings in Presence of Local Defects on Races" The Authors. Published by Elsevier Ltd. pp. 985-993.
[5]	Kanai, R. A., Desavale, R. G., and Chavan, S. P., 2016, "Experimental-Based Fault Diagnosis of Rolling Bearings Using Artificial Neural Network," ASME J. Tribol., 138(3), p. 031103.
[6]	Choy, F. K., Zhou, J., and Braun, M. J., 2005, "Vibration Monitoring and Damage Quantification of Faulty Ball Bearings," Trans. ASME, J. Tribol., 127, pp. 776–783.
[7]	Patil, M. S., Mathew, J., and Desai, S., 2010, "A Theoretical Model to Predict the Effect of Localized Defect on Vibrations Associated With Ball Bearings," Int. J. Mech. Sci., 52, pp. 1193–1201.
[8]	Desavale, R. G., Kanai, R. A., Chavan, S. P., Venkatachalam, R., Jadhav P. M.,2016 "Vibration Characteristics Diagnosis of Roller Bearing Using the New Empirical Model" ASME J. Tribol., Vol. 138 p. 011103
[9]	Desavale,R. G., 2019 "Dynamics Characteristics and Diagnosis of a Rotor-Bearing's System Through a Dimensional Analysis Approach: An Experimental Study" ASME Journal of Computational and Nonlinear Dynamics Vol. 14 p. 014501
[10]	Choudhury, A., Tandon, N.,1998 " A Theoretical Model to Predict Vibration Response of Rolling Bearings to Distributed Defects Under Radial Load" Transactions of the ASME Vol. 120 pp. 214-220